Subcortical Circuits Mediate Communication Between Primary Sensory Cortical Areas

Michael Lohse*[1], Johannes C. Dahmen[1], Victoria M. Bajo[1], Andrew J. King*[1]

[1]Department of Physiology, Anatomy, and Genetics. University of Oxford, Oxford OX1 3PT, United Kingdom.

*Correspondence should be addressed to M.L. (michael.lohse@dpag.ox.ac.uk) or A.J.K. (andrew.king@dpag.ox.ac.uk)

ACKNOWLEDGMENTS

The research was funded by a Wellcome Trust Studentship (WT105241/Z/14/Z) to M.L., and a Wellcome Trust Principal Research Fellowship (WT108369/Z/2015/Z) to A.J.K.

AUTHOR CONTRIBUTIONS

M.L. conceived and designed the research. M.L. performed research and analyzed the data. M.L. and J.C.D. performed surgeries. M.L. and A.J.K. acquired funding for the research. A.J.K. provided infrastructure and resources. A.J.K, J.C.D., and V.M.B. supervised the research. M.L., J.C.D., V.M.B. and A.J.K. interpreted the research. M.L., J.C.D., V.M.B. and A.J.K wrote the manuscript.

CONFLICT OF INTEREST

The authors declare no conflict of interest

Abstract

Integration of information across the senses is critical for perception and is a common property of neurons in the cerebral cortex, where it is thought to arise primarily from corticocortical connections. Much less is known about the role of subcortical circuits in shaping the multisensory properties of cortical neurons. We show that stimulation of the whiskers causes widespread suppression of sound-evoked activity in mouse primary auditory cortex (A1). This suppression depends on the primary somatosensory cortex (S1), and is implemented through a descending circuit that links S1, via the auditory midbrain, with thalamic neurons that project to A1. Furthermore, a direct pathway from S1 has a facilitatory effect on auditory responses in higher-order thalamic nuclei that project to other brain areas. Crossmodal corticofugal projections to the auditory midbrain and thalamus therefore play a pivotal role in integrating multisensory signals and in enabling communication between different sensory cortical areas.

Introduction

Having multiple sensory systems, each specialized for the transduction of a different type of physical stimulus, maximizes our ability to gather information about the external world. Furthermore, when the same event or object is registered by more than one sense, as is often the case, our chances of detecting and accurately evaluating its biological significance dramatically increase[1]. Unlike audition and vision, the sense of touch informs an organism exclusively about objects in its immediate vicinity. This is particularly important in animals that rely on their whiskers for detecting the presence and location of objects as they explore their surroundings[2]. Inputs from the whiskers can enhance sound-induced defensive behavior[3] and neural mechanisms that give precedence to the processing of somatosensory information over cues from other modalities are likely to be advantageous to the organism's survival.

Apart from specialized subcortical premotor nuclei, such as the superior colliculus, it is widely assumed that multisensory processing is most prevalent at the level of the cerebral cortex[1,4]. Evidence for multisensory convergence has been found in nearly all cortical areas, including the primary sensory cortices. In the primary auditory cortex (A1), for example, visual or tactile stimuli can modulate acoustically-driven activity, most commonly by suppressing responses to sound in both awake and anesthetized animals[5–8]. Suppression of sound-evoked activity in auditory cortical neurons by

31 somatosensory inputs likely provides a mechanism for prioritizing the processing of tactile cues from
32 nearby objects that require urgent attention.

33 The circuitry underlying crossmodal influences on processing in early sensory cortical areas is
34 poorly understood. Because visual, auditory and somatosensory cortices innervate each other and
35 connect with higher-level, association areas[5,7,9–14], most studies have focused on the role of
36 intracortical circuits in multisensory integration[15–18]. This, however, ignores the potential contribution
37 of ascending inputs from the thalamus, which may also provide a source of multisensory input to
38 primary cortical areas, such as A1[11,19–22], or the possibility that early sensory cortical areas may
39 communicate via a combination of corticofugal and thalamocortical pathways[23,24].

40 We show that somatosensory inputs exert a powerful influence on processing in the auditory
41 system, which is independent of brain state and takes the form of divisive suppression in the auditory
42 thalamus and cortex. Dissecting the underlying circuitry, we found that this suppression originates in
43 the primary somatosensory cortex (S1) and is implemented via S1-recipient neurons in the auditory
44 midbrain, which inhibit sound-driven activity in the auditory thalamocortical system. We also show
45 that a parallel crossmodal corticothalamic pathway from S1 to the medial sector of the auditory
46 thalamus allows for somatosensory facilitation of auditory responses in thalamic neurons that do not
47 project to the auditory cortex. These results demonstrate that the auditory midbrain and thalamus
48 have essential roles in integrating somatosensory and auditory inputs and in mediating
49 communication between cortical areas that belong to different sensory modalities.

50

51 Results

52 **Somatosensory influences on primary auditory cortex**

53 Because variable effects of tactile stimulation have been reported on the activity of neurons in the
54 auditory cortex of different species[6,7,25–27], we recorded extracellular activity in A1 of awake mice,
55 while presenting tones and simultaneously deflecting the whiskers (Figure 1a). We consistently found
56 that concurrent whisker stimulation reduced auditory responses (Figure 1a-c), demonstrating
57 widespread suppression of auditory activity in A1. Furthermore, assessment of the input-output
58 responses across all tones presented, normalized to the firing rate at each neuron's best frequency
59 (BF), revealed that this suppression was stimulus specific and of a divisive nature, with strong effects
60 around the BF and negligible effects for off-BF responses that were closer to baseline activity (Figure
61 1d,e). To assess whether the suppression was caused by non-sensory influences, such as stimulus-
62 triggered movements of the whiskers, changes in attention, or arousal, we also recorded from A1 of

anesthetized mice and obtained very similar results (Figure 2a-d). This indicates that the suppression of auditory responses by whisker stimulation is caused by an interaction between the somatosensory and auditory system that operates robustly across different brain states.

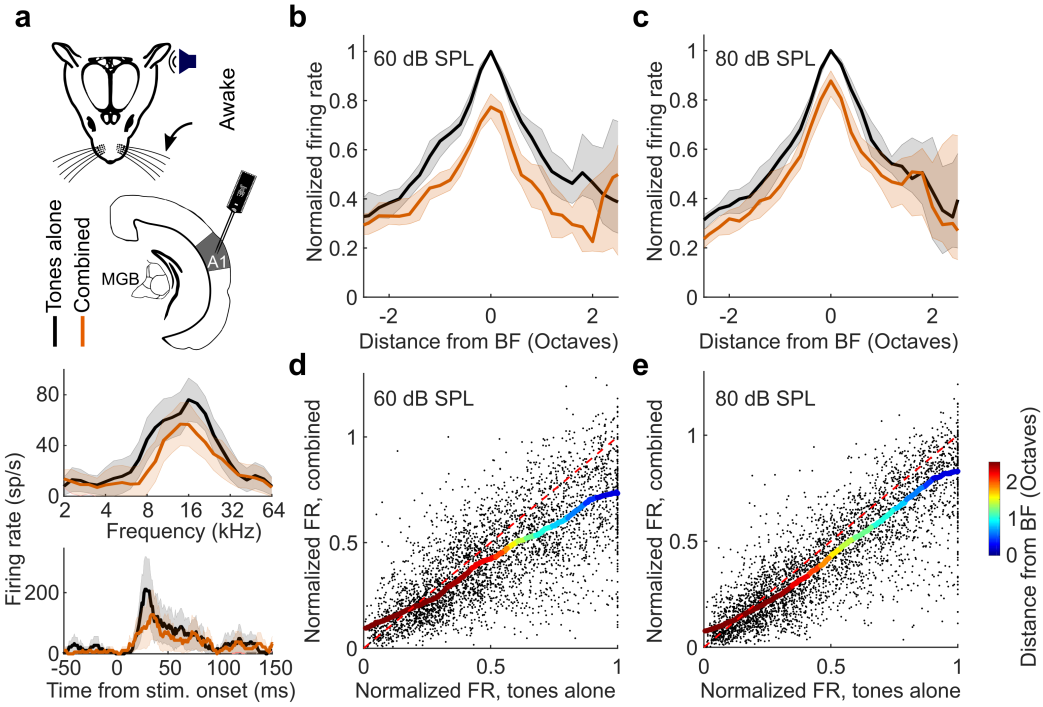

Figure 1. Somatosensory suppression of neurons in primary auditory cortex of awake, head-fixed mice. a *Top:* Schematic of recording setup. *Bottom:* Example frequency tuning curves and PSTHs of BF responses from a unit recorded in A1 of an awake, passively listening mouse, illustrating tone responses (80 dB SPL) with (orange) or without (black) concurrent whisker stimulation. **b**,**c** Median tuning curve for tones presented at 60 (**b**) and 80 dB SPL (**c**) across units recorded in A1 of awake mice (60 dB SPL change in BF response: $P < 0.001$, $n = 140$; 80 dB SPL change in BF response: $P < 0.001$, $n = 140$, Wilcoxon signed-rank test). **d**,**e** Relationship between normalized firing rate (FR) for all A1 units (black dots) for tones presented at 60 (**d**) or 80 dB SPL (**e**) across all frequencies either with ('combined') or without ('tones alone') whisker stimulation. Thick multi-colored lines show the running median of this relationship (window: 0.1 normalized firing rate), and the colors denote distance from BF. The diagonal dashed red line is the line of equality. A larger distance between the multi-colored line and the diagonal line at the blue end than at the red end indicates divisive scaling. Shaded area indicates the s.e.m. (**a**: *Bottom*), the 95% confidence intervals of the means (**a***: Top*), or the 95% nonparametric confidence intervals of the median (**b**,**c**). $n = 140$ (4 mice).

Somatosensory influences on auditory thalamus

To investigate the circuitry underlying this extensive modulation of auditory cortical processing, we first set out to determine whether the activity of subcortical auditory neurons is similarly affected by whisker stimulation. To maintain control over brain state and avoid self-generated movement of the whiskers during sensory stimulation, we carried out the majority of the circuit dissection experiments in anesthetized mice (unless specified otherwise). We found no evidence for somatosensory-auditory

interactions in the central nucleus of the inferior colliculus (CNIC) (Supplementary Fig. 1) and therefore focused on the medial geniculate body (MGB), the main thalamic gateway to the auditory cortex. We recorded from neurons in the lateral region of the MGB, including both the lemniscal ventral division (MGBv) and the non-lemniscal dorsal division (MGBd) (Fig. 2 and Supplementary Fig. 2). Whisker stimulation suppressed responses to noise and to tones near the BF of neurons in both MGBv and MGBd (Fig. 2a,e-g and Supplementary Fig. 3). As in the cortex, this suppression took the form of a divisive scaling of the sound-evoked response (Figure 2d,g). Similar somatosensory influences on auditory responses were found in MGBv/d of awake, head-fixed mice (Supplementary Fig. 4).

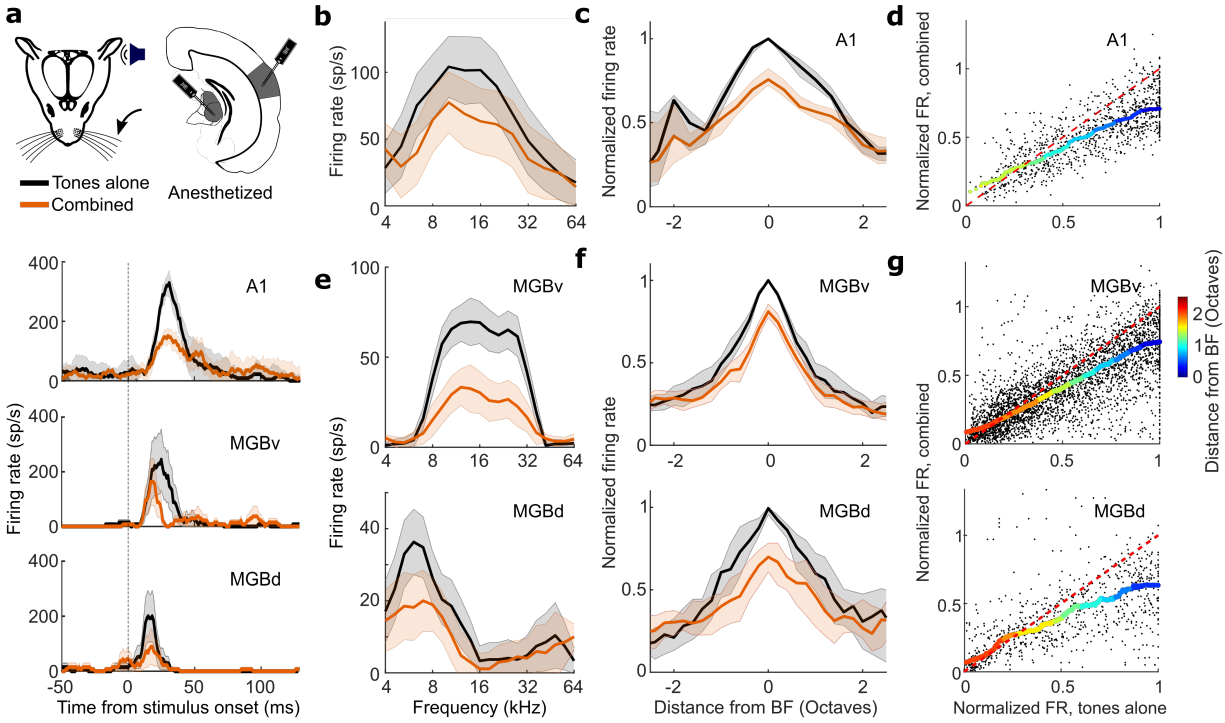

Figure 2. Divisive scaling of frequency tuning by somatosensation in A1, MGBv and MGBd of anesthetized mice. a *Top:* Schematic of recording setup. *Bottom:* Example PSTHs illustrating BF responses with (orange) or without (black) concurrent whisker stimulation from units in A1, MGBv and MGBd. **b** Example frequency tuning curves with or without concurrent whisker stimulation from the same A1 unit. **c** Median tuning curve across units recorded in A1 (change in BF response: $P < 0.001$, $n = 77$). **d** Relationship between normalized firing rate (FR) for all A1 units (black dots) for tones across all frequencies presented either with ('combined') or without ('tones alone') whisker stimulation. **e** Frequency tuning curves from the same MGB (*top:* MGBv, *bottom:* MGBd) units depicted in **a** either with or without concurrent whisker stimulation. **f** Median tuning curve across units recorded in MGBv (*top,* change in BF response: $P < 0.001$, $n = 145$) and MGBd (*bottom,* change in BF response, $P < 0.001$, $n = 31$) with or without concurrent whisker stimulation. **g** Relationship between normalized firing rate (FR) for all units (black dots) recorded in the MGBv (*top*) and MGBd (*bottom*) for tones across all frequencies presented either with ('combined') or without ('tones alone') whisker stimulation. **d**,**g** Thick multi-colored lines show the running median of this relationship (window: 0.1 normalized firing rate), and the colors denote distance from BF. The horizontal dashed red line denotes the median normalized spontaneous rate across units. The diagonal dashed red line is the line of equality. A larger distance between the multi-colored line and the diagonal line at the blue end than at the red end indicates divisive scaling. Shaded area indicates the s.e.m. (**a**), the 95% confidence intervals of the means (**b**,**e**), or the 95% nonparametric confidence intervals of the median

(**c**,**f**). n_{A1} = 77 (4 mice), n_{MGBv} = 145 (9 mice); n_{MGBd} = 31 (9 mice). See supplementary Fig. 4 for similar results in awake, head-fixed mice.

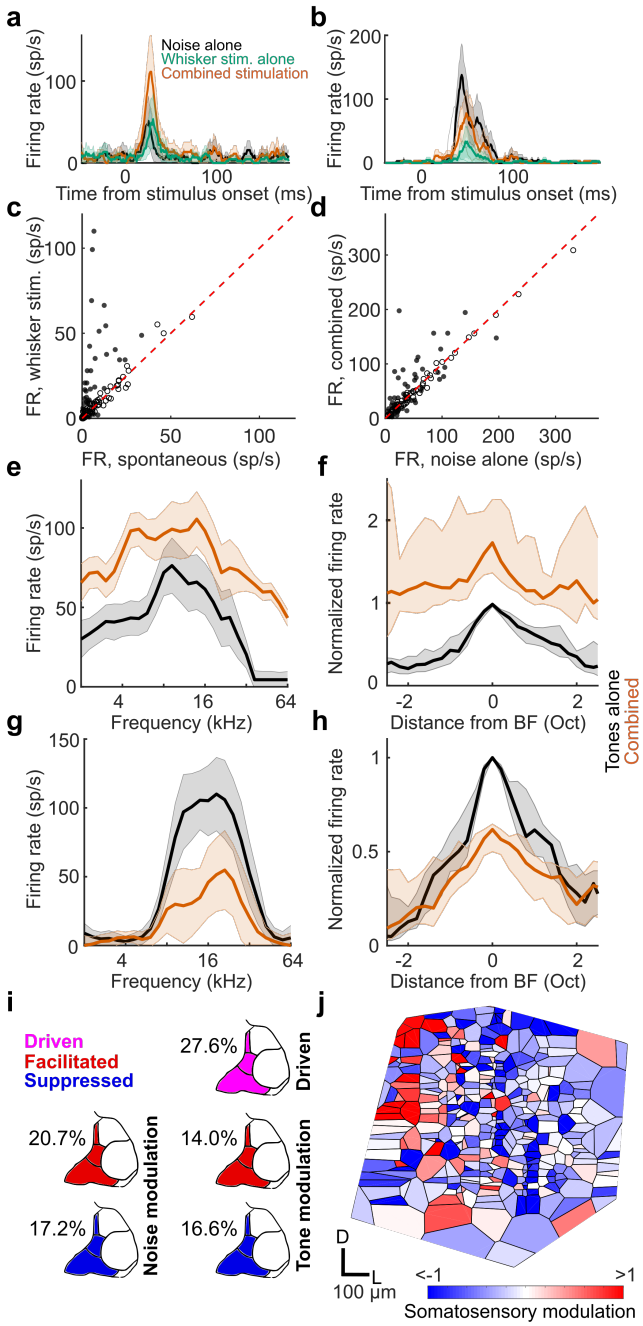

Figure 3. Diverse somatosensory influences on neurons in MGBm/PIN and SGN. a,**b** Example PSTHs of responses to broadband noise recorded in MGBm/PIN/SGN with (orange) and without (black) concurrent whisker stimulation, as well as to whisker stimulation alone (green), showing somatosensory facilitation (**a**, P < 0.05, *t*-test) and suppression (**b**, P < 0.05, *t*-test) of the auditory response, respectively. **c** Summary of responses (firing rate, FR) to whisker stimulation alone vs spontaneous activity in the medial sector of the auditory thalamus. Filled circles indicate units driven by somatosensory stimulation (P < 0.05, *t*-test). **d** Summary of responses to broadband noise combined with or without concurrent whisker stimulation. Filled circles indicate significantly (P < 0.05, *t*-test) modulated units (*n* = 116, 8 mice). **e** Example frequency tuning curves for tones with (orange) and without (black) concurrent whisker stimulation for a unit showing crossmodal facilitation (P < 0.05, *t*-test). **f** Summary tuning curves of units with significantly facilitated BF responses. **g**,**h** Same as **e**,**f** for units

with significantly suppressed BF responses. $n_{facilitated}$ = 32, $n_{suppressed}$ = 27, 12 mice. Shaded area indicates 95% confidence intervals of the mean (**a**,**b**,**e**,**g**) or nonparametric confidence intervals of the medians (**f**,**h**), respectively. **i** Percentage of neurons in the MGBm/PIN and SGN significantly (P < 0.05, one-sided *t*-test) driven by somatosensory input, or showing significant modulation (P < 0.05, two sided *t*-test) of the responses to noise or tones at BF when combined with somatosensory input. **j** Voronoi diagram illustrating somatosensory modulation in all tuned neurons across auditory thalamus. Each patch represents the location of one extracellularly recorded thalamic unit (*n* = 369, 14 mice) and is color-coded for the type and strength of somatosensory modulation (red, facilitation; blue, suppression). D, dorsal; L, lateral. See supplementary Fig. 5 for similar results in awake, head-fixed mice.

The medial section of the auditory thalamus contains several divisions, medial MGB (MGBm), the posterior intralaminar nucleus (PIN), and the suprageniculate nucleus (SGN), which are anatomically distinct from the MGBv and MGBd[28–30]. In the MGBm/PIN and SGN, we found that over a quarter (27.6%, a higher proportion than the 5% expected by chance, P < 0.001, binomial test) of noise-responsive units were directly driven (P < 0.05, *t*-test) by whisker inputs alone (Figure 3a,c,i). We also found that the responses of individual units to noise (Figure 3a,b,d,i) or tones (Figure 3e,f,g,h,i) could be either facilitated or suppressed when combined with whisker input. Units in which responses to tones were facilitated exhibited an increase in firing rate across the entire frequency tuning curve, indicative of additive scaling (Figure 3e,f), whereas suppressed units, similar to those in MGBv/d and cortex, showed divisive scaling (Figure 3g,h). Thus, neurons in the medial section of the auditory thalamus were influenced by whisker stimulation in a much more heterogeneous fashion than neurons in the lateral MGB (Figure 3j). We found similarly diverse modulations of auditory responses in MGBm/PIN and SGN in awake, head-fixed mice (Supplementary Fig. 5).

Somatosensory suppression of auditory cortex is inherited from the thalamus

Whisker-stimulation induced suppression of auditory activity is therefore present subcortically, particularly in the MGBv and MGBd, two auditory thalamic subdivisions with massive thalamocortical projections. This suggests that cortical neurons may inherit signals in which acoustic and somatosensory information have already been integrated. To investigate whether MGB neurons do indeed relay a whisker-modulated signal to auditory cortex, we expressed the calcium indicator GCaMP6m in the entire auditory thalamus and measured calcium transients in thalamocortical boutons in layer 1 of the auditory cortex[30] (Figure 4a,b). Layer 1 of the mouse auditory cortex tends to receive more diverse thalamic inputs than layers 3b/4. In A1, for example, layer 1 combines dense projections from MGBv[30,31] with projections from other structures, such as MGBm[30] and the lateral posterior nucleus of the thalamus[21]. Nevertheless, whisker stimulation had a suppressive effect on responses to both noise (Figure 4c,d) and tones (Figure 4e,f). Similar to neurons in MGBv, MGBd and

auditory cortex, frequency-tuned thalamocortical boutons exhibited divisive scaling with the largest response reduction at BF (Figure 4e,f). We did not find any auditory thalamocortical boutons that were driven by whisker stimulation alone or whose sound responses were facilitated by whisker stimulation. This suggests that only somatosensory suppression of auditory activity is projected to the auditory cortex, whereas the facilitation observed in the medial sector of the auditory thalamus is not.

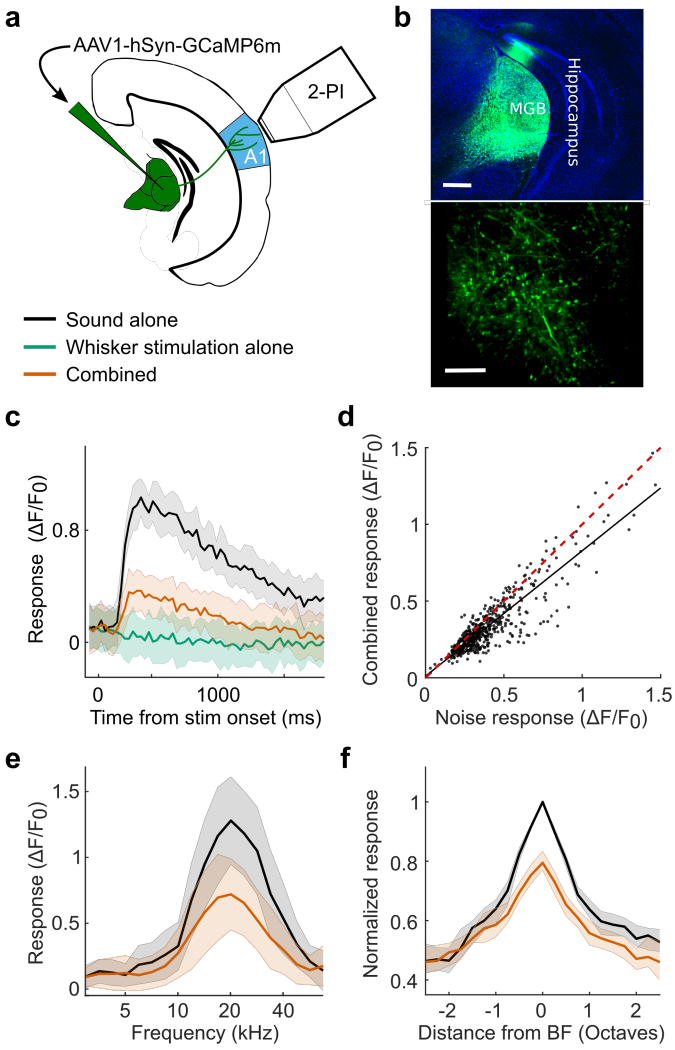

Figure 4: Thalamic inputs to auditory cortex are suppressed by whisker stimulation. a Schematic of recording setup. **b** *Top:* Confocal image of GCaMP6m expression in the auditory thalamus. Scale bar, 400 µm. *Bottom: In vivo* 2-photon image of thalamocortical boutons in layer 1 of the auditory cortex. Scale bar, 20 µm. **c** Calcium response of an example thalamic bouton in layer 1 responding to broadband noise with (orange) or without (black) concurrent whisker deflection, as well as to whisker deflection alone (green). **d** Summary of responses to noise alone vs combined noise plus whisker deflection in all noise-responsive thalamocortical boutons ($P < 0.001$, $n = 512$, 3 mice). The red dashed line indicates the line of equality. The black solid line indicates the least squares linear fit. **e** Frequency tuning curves with (orange) and without (black) whisker deflection from an example thalamocortical bouton. **f** Median frequency tuning curves across all frequency tuned boutons (change in BF response: $P < 0.001$, $n = 310$, 3 mice). Shaded area indicates the 95% confidence intervals of the means (**c**,**e**), or the 95% nonparametric confidence intervals of the median (**f**).

S1 mediates suppression of the auditory thalamus

To determine whether S1 is involved in whisker-stimulation induced suppression of the auditory thalamocortical system, we recorded neuronal activity in the MGB of VGAT-ChR2-YFP mice whilst silencing S1 optogenetically (Figure 5a and Supplementary Fig. 6). Silencing S1 did not affect spontaneous activity or tone-evoked auditory thalamic responses (Supplementary Fig. 6), but significantly reduced the capacity of whisker stimulation to suppress the BF responses of neurons in both MGBv and MGBd (Figure 5b,c). Thus, S1 is a critical part of the circuitry mediating the somatosensory control of auditory thalamocortical responses.

Silencing S1 also had a similar effect on the responses of neurons in the medial sector of the auditory thalamus that were otherwise robustly suppressed by whisker stimulation (Supplementary Fig. 7), but did not affect the capacity of whisker stimulation to enhance responses in this part of the thalamus (Supplementary Fig. 7). S1 is thus necessary for somatosensory suppression throughout the auditory thalamus, but not for somatosensory facilitation. That S1 activation is also sufficient for the suppression of auditory thalamocortical responses was revealed when we optogenetically activated infragranular cells in S1 via the red-shifted opsin ChrimsonR and measured calcium transients in thalamocortical boutons (Figure 5d,e). Optogenetic S1 activation suppressed their responses to noise bursts (Figure 5f,g) and thus replicated the previously observed whisker-induced suppression of auditory thalamocortical boutons.

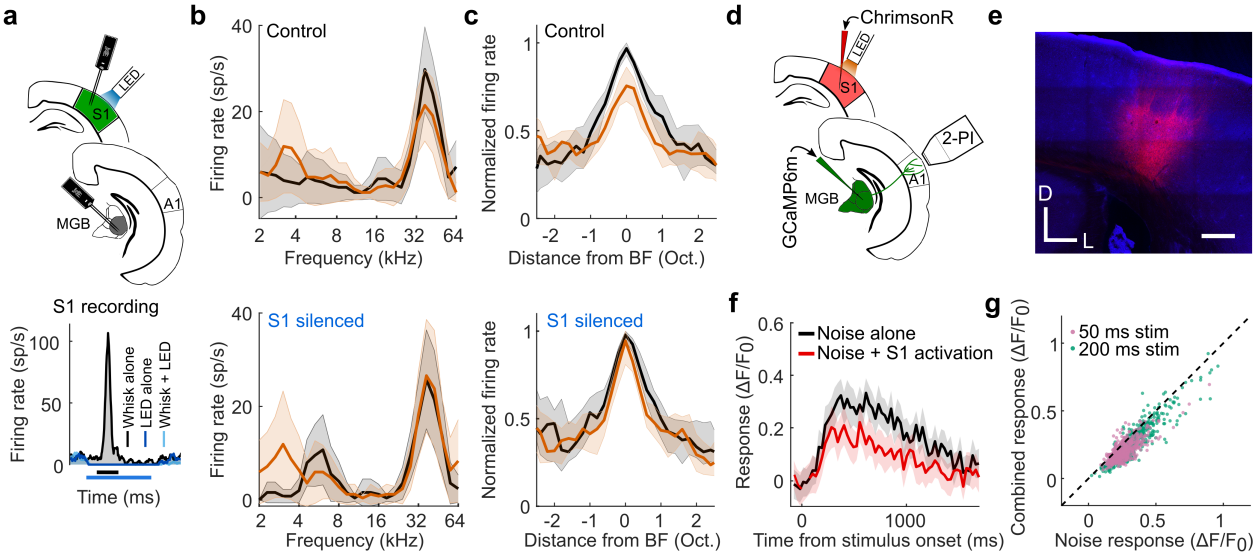

Figure 5: S1 mediates somatosensory suppression of auditory thalamocortical axons. a *Top:* Schematic of optogenetic targeting of somatosensory cortex in VGAT-ChR2 mice and electrophysiological recording setup. *Bottom:* Example PSTHs of a unit recorded in S1, demonstrating the effect of optogenetic silencing of

202 somatosensory cortex on spontaneous activity and whisker-stimulation evoked responses. Bars below the x-axis
203 indicate timing of whisker stimulation (black) and photostimulation for silencing S1 (blue). **b** Frequency tuning
204 curves of an example MGBv unit based on tone responses with (orange) and without (black) concurrent whisker
205 stimulation during the control condition (top) and when S1 was silenced (bottom). **c** Median tuning curves of all
206 units recorded in MGBv/d with (orange) and without whisker deflection (black) during the control condition
207 (top) and when S1 was silenced (bottom). The suppressive effect of whisker stimulation on the BF response of
208 MGBv/d neurons was reduced following S1 silencing (P = 0.014, *n* = 59, 3 mice). **d** Schematic of experimental
209 setup for combined 2-photon thalamocortical bouton imaging with optogenetic activation of S1. **e** Confocal
210 image showing expression of ChrimsonR-tdTomato in infragranular layers of S1. Scale bar, 300 µm. D, dorsal; L,
211 lateral. **f** Calcium response of an example thalamic bouton in layer 1 of the auditory cortex, illustrating
212 suppression of the response to a 50 ms noise burst by optogenetic S1 stimulation. Shading indicates 95%
213 confidence intervals around the mean. The 3rd and 4th imaging frames of the S1 stimulation condition displayed
214 a large light artefact from the LED and have therefore been removed. **g** Summary plot of responses to noise
215 alone or noise combined with infragranular S1 stimulation for all noise-responsive boutons. Purple and green
216 points indicate responses to 50 ms and 200 ms noise stimulation, respectively. n_{50ms} = 539, 8 imaging fields, 1
217 mouse; n_{200ms} = 652, 7 imaging fields, 2 mice. Shaded area indicates the 95% confidence intervals of the means
218 (**b**,**f**), or the 95% nonparametric confidence intervals of the median (**c**).

219 **Auditory cortex does not mediate somatosensory influences on auditory thalamus**

220 One way in which S1 could suppress neuronal activity in the auditory thalamus is via an indirect
221 corticocorticothalamic route that takes advantage of the massive corticothalamic projections
222 originating in the auditory cortex. However, although silencing auditory cortex strongly decreased
223 both spontaneous activity (Supplementary Fig. 6) and sound-evoked responses in MGBv and MGBd
224 neurons (Supplementary Fig. 8), this did not alter the suppressive effects of whisker stimulation on
225 the responses of these neurons or the facilitatory influence of whisker stimulation on neurons located
226 in the medial sector of the auditory thalamus (Supplementary Fig. 8).

227

228 **S1 projection neurons account for auditory thalamic facilitation**

229 To investigate whether a direct corticothalamic projection[24,32,33] exists that could mediate
230 somatosensory control over auditory thalamus, we performed viral tracing experiments in S1
231 corticothalamic neurons. These revealed that a projection does indeed exist, which originates from
232 RBP4-expressing layer 5 neurons in S1 and densely innervates the medial sector of auditory thalamus
233 (Figure 6a-c), particularly the PIN (Figure 6b,c). Optical stimulation of these S1 layer 5 neurons
234 significantly altered the spontaneous firing rate of more than a third of recorded units (Figure 6d,e),
235 suggesting a direct excitatory pathway from S1 to the medial auditory thalamus. Activation of this
236 pathway also replicated the additive scaling of the frequency response profiles of auditory neurons
237 recorded in this region of the auditory thalamus (Figure 6f,g) that we observed when combining
238 sounds and whisker stimulation.

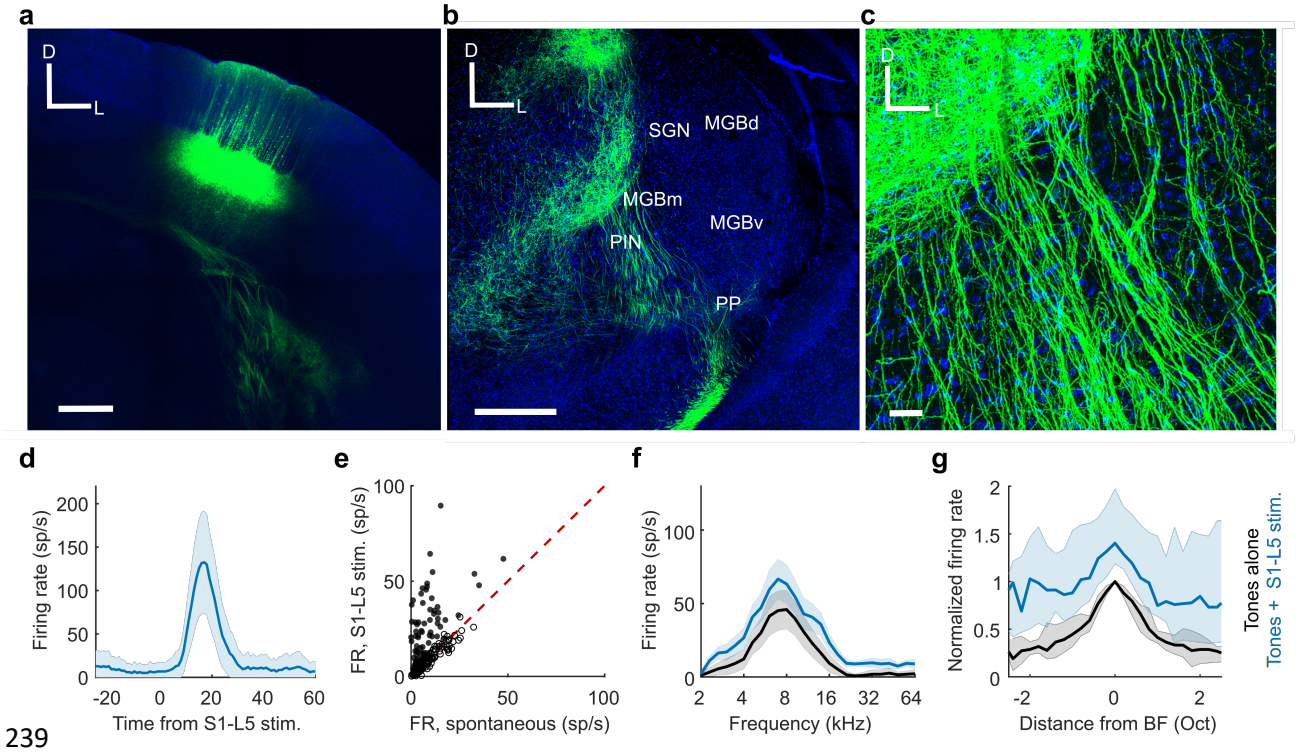

Figure 6: Direct pathway from S1 to MGBm/PIN and SGN. a Confocal image of ChR2-YFP expression in RBP4+ cells in layer 5 (L5) of S1. Scale bar, 400 µm; D, dorsal; L, lateral. **b** Confocal image of a coronal section of the thalamus showing S1-L5 (RBP4+) axons in the medial sector of the auditory thalamus. PP, peripeduncular nucleus. Scale bar, 400 µm. **c** High magnification image showing S1-L5 (RBP4+) axons in MGBm/PIN. Blue = DAPI, Green = YFP. Scale bar, 30 µm. **d** Example unit located in MGBm/PIN that was driven by stimulation of S1-L5 (RBP4+) neurons. **e** Summary of MGBm/PIN neuronal firing rate (FR) responses to 50 ms light pulses delivered to stimulate S1-L5 (RBP4+) neurons. n = 183, 5 mice. Filled circles indicate the 69 units in which spontaneous firing was significantly altered ($p < 0.05$, t-test) by S1-L5 stimulation. **f** Tuning curves from an example unit in MGBm/PIN in which the auditory response was significantly enhanced by concurrent stimulation of S1-L5 (RBP4+) neurons. **g** Median tuning curves from units in the medial sector of auditory thalamus with significantly ($P < 0.05$, t-test) facilitated BF responses during stimulation of S1-L5 (RBP4+) neurons. n = 25, 5 mice. Shaded areas indicate the s.e.m. (**d**), the 95% confidence intervals of the means (**f**) or the 95% nonparametric confidence intervals of the medians (**g**), respectively. BF responses were significantly modulated in 18% (13.7% facilitated, 4.4% suppressed; n = 183, 5 mice) of units in MGBm/PIN and SGN by concurrent stimulation of S1-L5 (RBP4+) neurons.

Although these findings are consistent with a facilitatory influence of layer 5 projection neurons in S1 on neurons in the medial auditory thalamus, selective stimulation of the RBP4-expressing neurons did not induce suppression of the sound-evoked responses of neurons recorded in the MGBv and MGBd (Supplementary Fig. 9). This result can be readily accounted for given the generally excitatory nature of corticofugal projections and the predominantly medial termination pattern of this particular pathway, as well as the relative paucity of GABAergic interneurons in the rodent MGB[34]. Nevertheless, the lack of effect from stimulation of S1 RBP4-expressing neurons on the

sound-evoked responses of neurons recorded in the lateral auditory thalamus contrasts with the reduced influence of whisker stimulation on those responses when S1 was silenced optogenetically. This therefore implies the existence of another pathway by which S1 neurons can influence auditory processing in this part of the thalamus.

A corticocollicular pathway for somatosensory thalamic suppression

The final objective was to identify the source of inhibition mediating S1-dependent suppression of neuronal activity in the auditory thalamus. One major source of inhibitory input to the MGB, and a structure that has previously been implicated in crossmodal thalamic processing[35], is the thalamic reticular nucleus (TRN). By optogenetically silencing the auditory sector of TRN (AudTRN) during tone presentation, we found that this part of the thalamus modulates the excitability of MGB neurons (Figure 7a-c). Surprisingly, however, we did not find any evidence that AudTRN neurons play a role in mediating somatosensory suppression of the MGB (Figure 7d,e).

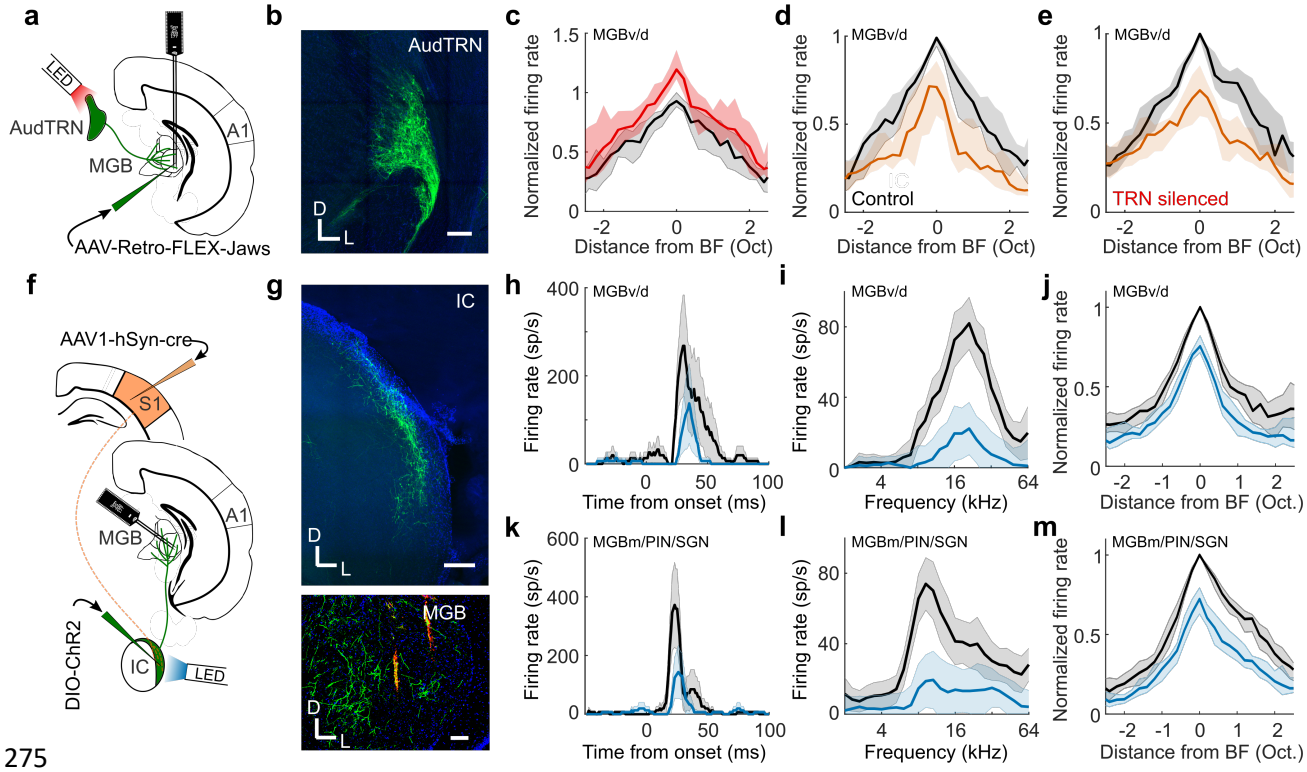

Figure 7: Corticocollicular circuit mediates somatosensory suppression of the thalamus. a Schematic of experimental paradigm in **b**-**e**. **b** GABAergic cells in TRN retrogradely-labelled with Jaws from auditory thalamus. Scale bar, 150 µm. **c** Summary (median) frequency tuning curve across MGBv/d units with (red) or without (black) optogenetic suppression of AudTRN activity (change in BF firing response, $P < 0.001$, $n = 38$, 2 mice). **d**,**e** Median frequency tuning curve of MGBv/MGBd units illustrating suppression induced by concurrent whisker stimulation (orange) with AudTRN either unaffected (**d**) or optogenetically silenced (**e**). Silencing AudTRN had no effect on the whisker-induced suppression of auditory responses in MGBv/MGBd ($P = 0.83$, $n = 38$, 2 mice). **f** Schematic of experimental paradigm in **g**-**m**. **g** *Top:* ChR2-YFP expression in neurons in the shell of IC, labelled by anterograde transport of cre from S1 (AAV1-hSyn-cre) and a cre-dependent AAV5-DIO-ChR2-eYFP injected into

the IC. Scale bar, 200 µm. *Bottom:* Axons (green) of anterogradely labelled IC neurons in MGB. Scale bar, 100 µm. Orange marks show DiI tracts from the recording probe in the MGB. D, dorsal; L, lateral. **h** Example PSTHs illustrating BF responses of an MGBv unit with (blue) and without (black) optogenetic stimulation of S1-recipient IC neurons. **i** Example frequency tuning curve of an MGBv unit with (blue) and without (black) optogenetic stimulation of S1-recipient IC neurons. **j** Median MGBv/MGBd tuning curve with (blue) and without (black) stimulation of S1-recipient IC neurons: -20.9% median change in BF firing rate ($P < 0.001$; $n = 85$, 3 mice). **k-m** same as **h-j** for units recorded in MGBm/PIN/SGN. **m** -26.9% median change in BF firing rate ($P < 0.001$; $n = 89$, 3 mice). Shaded area illustrates the s.e.m. (**h**,**k**), the 95% confidence intervals of the means (**i**,**l**), or the 95% nonparametric confidence intervals of the median (**c**,**d**,**e**,**j**,**m**).

Inhibitory input to the MGB can also arrive from extra-thalamic sources, including the IC[36–38], which provides its major source of ascending input. Interestingly, descending inputs from the somatosensory cortex appear to target modular zones containing GABAergic neurons within the lateral shell of the mouse IC[36], suggesting a possible route by which whisker stimulation could influence auditory processing. In order to selectively target IC neurons that receive input from S1, we employed an anterograde transsynaptic viral tagging approach[39], which involved injecting AAV1-hSyn-cre into S1. Combining this with an injection into the IC of a virus that cre-dependently expresses both channelrhodopsin-2 and eYFP, we were able to show that S1 targets a subset of IC shell neurons (Figure 7f,g) and that these neurons project to the auditory thalamus (Figure 7g). Furthermore, activating these S1-recipient IC neurons induced suppression of auditory responses both in MGBv/d (Figure 7h-j) and the medial auditory thalamus (Figure 7k-m). This demonstrates that S1 exerts suppressive control over auditory thalamic processing via a corticocolliculothalamic pathway, in addition to its facilitatory influence via a direct crossmodal corticothalamic pathway (Figure 8).

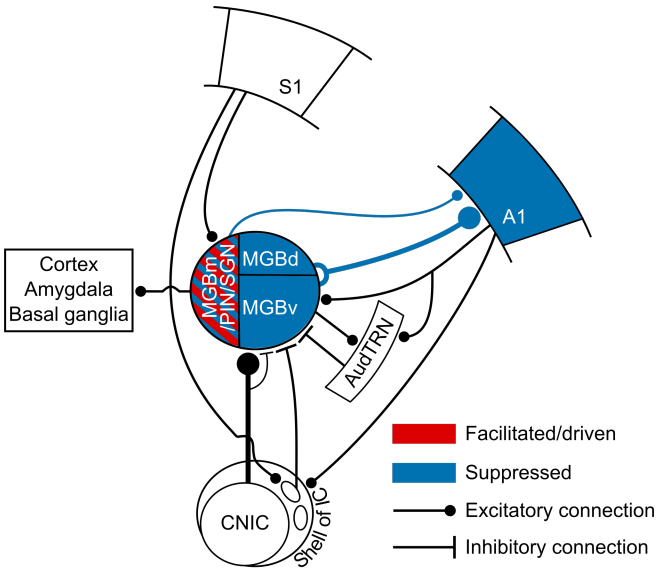

Figure 8: Circuits enabling somatosensory control of the auditory thalamocortical system. Auditory responses in the regions of the auditory thalamus and cortex depicted in blue were suppressed by concurrent whisker stimulation via a descending pathway from S1 to the lateral shell of IC, which then projects to the MGB. Some neurons in the medial sector of the auditory thalamus were driven or had their auditory responses enhanced by whisker stimulation (depicted in red), which can be mediated by a direct corticothalamic projection from S1 to MGBm/PIN/SGN.

Discussion

Our results demonstrate that the somatosensory system exerts a powerful influence over sound processing in both the auditory cortex and thalamus. These effects are diverse and anatomically specific. We identified two separate corticofugal pathways (Figure 8), which both originate in S1 but exert opposing somatosensory control over the auditory thalamus. First, a crossmodal descending pathway via the auditory midbrain mediates somatosensory divisive suppression in the auditory thalamocortical system. Second, a direct corticothalamic pathway targets the medial sector of auditory thalamus, through which S1 drives spiking activity and facilitates neuronal responses that are not transmitted to the auditory cortex. These findings therefore reveal an unexpected role for corticofugal projections to both the auditory midbrain and thalamus in shaping the multisensory properties of auditory cortical and other downstream neurons and in enabling communication between different cortical areas.

Auditory cortex inherits multisensory signals from the thalamus

Multisensory interactions occur throughout the cerebral cortex, including early sensory areas[1,4]. Although spiking responses to visual or somatosensory stimuli have been found in different parts of auditory cortex, the commonest type of crossmodal interaction is seen in studies that paired otherwise ineffective stimuli with a sound[5–8,18,25,26,40,41]. Diverse modulatory effects on auditory cortical processing have been reported in these studies, and, in line with our results, several have found that crossmodal suppressive interactions are particularly prevalent, both in rodents[6,21,27] and other species[5,7,8,42].

The search for the source of these non-auditory influences on auditory cortical activity has focused principally on other cortical areas. Direct connections between early sensory cortical areas have been widely reported in different species[5,7,9–13]. Furthermore, in mice, optogenetic stimulation of A1 corticocortical projections can modulate the activity[15,16] and stimulus selectivity[16] of neurons in primary visual cortex via local inhibitory circuits. These studies therefore highlight the importance of intracortical connections in mediating multisensory interactions.

340 Non-auditory influences on auditory cortical processing can also be inherited from the
341 thalamus. Anatomical studies have emphasized the potential contribution to multisensory processing
342 in the auditory cortex of extralemniscal thalamic input, not just from non-primary regions of the MGB,
343 such as the MGBm, but also from areas like the SGN and the pulvinar[11,43,44]. Indeed, in mice, the
344 suppressive effects of visual looming stimuli on A1 activity appear to be mediated by the lateral
345 posterior nucleus, the rodent homologue of the primate pulvinar[21]. However, A1 receives the great
346 majority of its ascending input from the MGBv, which is traditionally viewed as a unisensory structure.
347 Nevertheless, cutaneous electrical stimulation has been shown to modulate auditory responses in the
348 MGBv[19,22], and our findings demonstrate that the sound-evoked responses of most neurons recorded
349 there and in the MGBd are suppressed by concurrent whisker stimulation. Moreover, we observed
350 comparable crossmodal suppression in auditory thalamocortical axon boutons and in A1 neurons,
351 indicating that somatosensory-auditory interactions are likely inherited by these cortical neurons from
352 their primary source of thalamic input.

353 In the MGBv and MGBd, the strongest suppressive effects induced by whisker stimulation
354 occurred at the BF of the neurons, i.e. the tone frequency at which the largest response was obtained.
355 This crossmodal divisive scaling by non-driving sensory inputs resembles that found in primate
356 cortex[45–47]. The divisive normalization operating in these areas is thought to be a canonical feature of
357 multisensory integration, which can account for the way neuronal responses depend on the efficacy
358 and spatial relationship of the individual stimuli[46]. Our results suggest that this may be a more
359 widespread property of multisensory neurons, even occurring in a structure (i.e. the auditory
360 thalamus) that lacks recurrent connectivity[48].

361 In contrast to the exclusively suppressive effects of somatosensory stimulation on the MGBv
362 and MGBd, neurons in the medial sector of the auditory thalamus (MGBm, PIN and SGN) exhibited a
363 mixture of crossmodal suppression and enhancement and more than a quarter were driven by whisker
364 stimulation. Somatosensory responses have previously been reported in these areas in other
365 species[49,50]. The facilitatory effects of whisker deflection were replicated by optogenetic activation of
366 S1 layer 5 neurons, but were preserved when S1 was silenced. This suggests that they reflect a
367 convergence of top-down corticothalamic and bottom-up inputs from spinothalamic, dorsal column
368 and trigeminal pathways[51–53]. Neurons in these medial thalamic structures primarily target secondary
369 auditory and higher-level association cortical areas, and the minority that innervate A1 terminate in
370 layer 1 and layer 5/6[30,54,55]. However, the thalamic axon boutons that we imaged in layer 1 showed
371 exclusively crossmodal suppression of sound-evoked activity, suggesting that neurons whose
372 responses are facilitated somatosensory inputs project elsewhere in the brain. Their targets include

373 the basal ganglia[30,56] and amygdala[30,50,54,57], with the latter projection being a critical part of the
374 circuitry mediating auditory fear conditioning[57–59].

375 In addition to differences in their efferent targets and in the effects of somatosensory inputs
376 on their responses to sound, the physiological properties of neurons in the MGBm, PIN and SGN are
377 distinct in other ways from those in the MGBv/MGBd[60]. Indeed, the lack of excitatory connectivity
378 between these neurons[48] makes the auditory thalamus an ideal place to establish functionally distinct
379 pathways that are independently and flexibly modulated by contextual information, including inputs
380 from other senses or motor commands[24].

381 **Corticofugal crossmodal control of the auditory thalamus**

382 There is growing evidence that descending corticofugal pathways contribute to the processing of
383 sensory information, both within and across sensory modalities, and to integrating sensory and motor
384 signals[24,32,33,61,62]. We found that activity in S1 can modulate sound-evoked responses throughout the
385 auditory thalamus, and therefore in the auditory cortex, demonstrating the existence of a trans-
386 thalamic pathway for mediating the influence of somatosensory stimuli on auditory cortical
387 processing. Although auditory cortical feedback can inhibit MGB activity via GABAergic neurons in the
388 TRN[63], this pathway does not appear to be involved in the somatosensory suppression of auditory
389 responses. Instead, this depends on a descending projection from S1 to IC shell neurons that inhibit
390 responses in the MGB. Somatosensory dominance over auditory processing in mouse A1 is therefore
391 implemented by a corticocolliculo-thalamocortical circuit. These findings add to the growing evidence
392 that trans-thalamic circuits enable communication between different cortical areas[23], and
393 demonstrate that the midbrain is also part of the circuitry responsible for integrating multisensory
394 signals across the cerebral cortex.

395 Interactions between somatosensory and auditory inputs occur as early as the cochlear
396 nucleus in the brainstem[64]. We did not observe any effects of whisker stimulation on the auditory
397 responses of neurons recorded in the CNIC, the primary relay nucleus of the auditory midbrain,
398 suggesting that multisensory suppression in the MGBv is unlikely to be inherited from earlier in the
399 auditory pathway. However, the lateral shell of the IC receives somatosensory inputs from much of
400 the body via projections from the somatosensory cortex and the brainstem[36,65]. In mice, these inputs
401 target GAD-67-positive modules that are separated by regions receiving auditory inputs[36].
402 Furthermore, GABAergic neurons throughout the IC project to the MGB[37,38,66,67]. Our data therefore
403 bridge these anatomical studies and establish a functional role for such circuits by demonstrating that
404 a relatively small population of S1-recipient neurons in the lateral shell of the IC are responsible for
405 the suppressive effects of whisker stimulation on sound-evoked responses in the auditory thalamus.

Perceptual implications of somatosensory control over auditory processing

Given its key position in the sensory and motor systems of the brain, context-dependent modulation of neuronal activity in the thalamus has wide-ranging consequences for information processing, not only in the cerebral cortex but also in other thalamorecipient brain regions, such as the amygdala and basal ganglia. The presence of region-specific multisensory interactions throughout the auditory thalamus therefore implies that combining information from different sensory modalities at this relatively early stage in the processing hierarchy plays a fundamental role in how animals perceive and interact with their sensory environments.

In rats, facial touch is associated with inhibition of the auditory cortex[6], potentially reflecting a greater salience of haptic information during social interactions and exploration. Our data suggest that these effects are likely to be present in the thalamus too and that they are asymmetric since we observed a much weaker modulatory influence of sound on neuronal responses to whisker stimulation in the somatosensory thalamus and no effect on whisker responses in the barrel field of S1 (Supplementary Fig. 10). The suppressive effects of somatosensory stimulation on sound-evoked responses, which have now been reported at multiple stages of the auditory pathway, may also help to reduce the impact of vocalizations or other self-generated and potentially distracting sounds, such as those resulting from chewing or breathing[4].

Although somatosensory suppression of auditory thalamocortical activity may reflect the relative importance of these inputs when nearby objects are encountered during exploration of the environment, a reduction in the firing rate of auditory neurons in the presence of other sensory cues can be accompanied by an increase in response reliability and in the amount of stimulus-related information transmitted[5,68]. Furthermore, auditory cortical activity is suppressed when an animal engages in a task[69]. Of particular relevance to the present study is the finding that divisive scaling of auditory cortical frequency tuning, as demonstrated in our recordings, is associated with improved frequency discrimination at the expense of impaired tone detection[62]. By inducing divisive gain in the auditory thalamocortical system, somatosensory inputs might function as a bottom up cue that sharpens auditory acuity, whilst reducing sensitivity.

Data availability

All relevant data are available on request to, and will be fulfilled by, the lead contact (michael.lohse@dpag.ox.ac.uk).

Code availability

Matlab code for analyses are available on request to, and will be fulfilled by, the lead contact (michael.lohse@dpag.ox.ac.uk).

Methods

Mice

All experiments were approved by the Committee on Animal Care and Ethical Review at the University of Oxford and were licensed by the UK Home Office (Animal Scientific Procedures Act, 1986, amended in 2012). Four strains of male and female mice were used: *C57BL6/J* (Envigo, UK), *VGAT-ChR2-YFP* (JAX 014548 - Jackson Laboratories, USA), *VGAT-cre* (JAX 016962 - Jackson Laboratories, USA), and *C57BL6/NTac.Cdh23*. *C57BL6/J*. *C57BL6/J, VGAT-ChR2-YFP*, and *VGAT-cre* mice were 7–12 weeks old, and *C57BL6/NTac.Cdh23* mice[70] were 10–20 weeks old at the time of data collection. All experiments were carried out in a sound-attenuated chamber.

Stimuli

Auditory stimuli were programmed and controlled in custom-written Matlab code (https://github.com/beniamino38/benware) and generated via TDT RX6 (electrophysiology) or RZ6 (2-photon imaging) microprocessors. Sounds were generated at a ~200 kHz sampling rate, amplified by a TDT SA1 stereo amplifier and delivered via a modified (i.e. sound was 'funnelled' into an otoscope speculum) Avisoft ultrasonic electrostatic loudspeaker (Vifa - electrophysiology) or a TDT EC1 electrostatic speaker (imaging) positioned ~1 mm from the entrance to the ear canal. The sound presentation system was calibrated to a flat (±1 dB) frequency-level response between 1 and 64 kHz. Stimuli included pure tones, covering a frequency range from 2 to 64 kHz, and broadband noise bursts (1-64 kHz). All sounds included 5-ms linear amplitude onset/offset ramps, and unless specified otherwise were presented at 80 dB SPL.

Whisker deflections were delivered with a piezoelectric bimorph attached to a small glass tube. During stimulation, the majority of the whiskers were either positioned inside the stimulation tube (anesthetized recordings), or a small brush with plastic hairs was attached to the tube in which whiskers were interspersed in the hairs of the brush (awake recordings). We deflected the whiskers in a single cosine wave (valley-to-valley), transiently displacing the whiskers 1 mm from resting position at a speed of 40 mm/s.

466 Presentation of acoustic and whisker stimuli was randomly interleaved, with each sensory
467 stimulus having a duration of 50 ms, unless otherwise specified.

468 ## Extracellular recordings

469 We carried out extracellular recordings using 32- or 64-channel silicon probes (NeuroNexus
470 Technologies Inc.) in a 4 × 8, 8 × 8 or 2 × 32 electrode configuration. Prior to insertion, probes were
471 coated with DiI (Sigma-Aldrich) for subsequent histological verification of the recording sites. Data
472 were acquired using a RZ2 BioAmp processor (TDT) and custom-written Matlab code
473 (https://github.com/beniamino38/benware).

474 For recordings under anesthesia, mice were anesthetized with an intraperitoneal injection of
475 ketamine (100 mg kg^{-1}) and medetomidine (0.14 mg kg^{-1}). Intraperitoneal injections of atropine
476 (Atrocare, 1 mg kg^{-1}) to prevent bradycardia and reduce bronchial secretions and dexamethasone
477 (Dexadreson, 4 mg kg^{-1}) to prevent brain edema were administered. Prior to the surgery, the analgesic
478 bupivacaine was injected under the scalp. The depth of anesthesia was monitored via the pedal reflex
479 and adjusted via small additional doses of the ketamine/medetomidine mix (1/5th of the initial dose)
480 given subcutaneously approximately every 15 min once the recordings had started (~1–1.5 h post
481 induction of anesthesia). A silver reference wire was positioned in the visual cortex of the contralateral
482 hemisphere and a grounding wire was attached under the skin on the neck musculature. The head
483 was fixed in position with a metal bar attached to the skull with dental adhesive (Super Bond C&B).

484 For awake recordings in the auditory thalamus and auditory cortex, we implanted a
485 recording chamber under isoflurane (1.5–2% in O_2) general anesthesia. Mice were administered
486 buprenorphine (Vetergesic 1 ml/kg), dexamethasone (Dexadreson 4 µg), and atropine (Atrocare 1
487 µg) intraperitoneally. An additional dose of buprenorphine was given 24 hours post-operatively. The
488 recording chamber consisted of a well that was constructed out of dental adhesive (Super Bond
489 C&B) encircling the craniotomy, which was sealed with a circular glass window. We positioned the
490 recording chamber either above the visual cortex (centered ~3 mm caudal from bregma and
491 ~2.1 mm lateral from midline) for auditory thalamus recordings, or above A1, together with a head
492 bar, and placed a reference electrode (silver wire) in the contralateral hemisphere. One or two days
493 later the mouse was head-fixed, the recording chamber opened, and a sterile recording probe
494 acutely inserted into the brain via the recording chamber.
495
496 All recordings were performed in the right hemisphere. In the anesthetized preparation,
497 circular craniotomies (2 mm diameter) were performed above the IC (centered ~5 mm posterior from
498 bregma and ~1 mm lateral from midline), over the visual cortex for auditory thalamic recordings

499 (centered ~3 mm caudal from bregma and ~2.1 mm lateral from midline), and/or over A1 (centered
500 ~2.5 mm posterior from bregma and ~4.5 mm lateral from midline). The exposed dura mater was kept
501 moist with saline throughout the experiment.

502 Recording sites were considered to be in the CNIC when the units recorded on those sites
503 were part of a clear dorso-ventral tonotopic gradient[71,72] and the probe's location could be confirmed
504 by post-mortem brain histology. For recordings in the MGB, probe sites were attributed to specific
505 auditory thalamic subdivisions by histological reconstruction of the recording sites (Supplementary
506 Figure 2). We parcellated the auditory thalamus based on previous immunohistochemical
507 descriptions[28] and our own pilot tracing experiments from several cortical areas. Accordingly,
508 recording sites were assigned to the ventral division (MGBv), dorsal division (MGBd), medial division
509 and posterior intralaminar nucleus (MGBm/PIN), or suprageniculate nucleus (SGN). Based on these
510 histological reconstructions, recording sites attributed to the MGBv were located <500 µm from the
511 lateral border of the MGB and <500 µm from the deepest acoustically-responsive site, while those in
512 the MGBd were <500 µm from the lateral border of the MGB, but >500 µm from the most ventral
513 acoustically-responsive site. For recordings in the medial sector of the auditory thalamus, sites
514 assigned to the MGBm/PIN were >500 µm from the lateral border of the MGB and <500 µm from the
515 most ventral acoustically-responsive site, and those in the SGN were >500 µm from the lateral border
516 of the MGB and >500 µm from the most ventral acoustically-responsive site.

517 A1 was identified by robust neuronal responses to broadband noise bursts, well-tuned
518 neurons, and a well-defined caudo-rostral tonotopic axis[30,73]. Cortical tonotopy was assessed in all
519 anesthetized cortical recordings by estimating frequency response areas from responses to pure tones
520 using probes with four recording shanks spaced 200 µm apart and oriented parallel to the caudo-
521 rostral axis. Recordings in awake animals were performed in positions corresponding to those
522 identified as A1 from the anesthetized cases.

523 Two-photon calcium imaging of thalamocortical boutons

524 All injections were performed using a custom-made pressure injection system with a calibrated glass
525 pipette positioned in the right hemisphere. We made injections of ~140 nl (diluted 1:1 in PBS) of
526 AAV1.Syn.GCaMP6m.WPRE.SV40 into the auditory thalamus (3 mm caudal from bregma, 2.1 mm
527 lateral from midline and 2.8 - 3 mm ventral from the cortical surface) for expression of GCaMP6m in
528 auditory thalamic neurons and axons as reported previously[30].

529 In order to visualize the calcium activity of thalamic boutons in layer 1 (20-80 µm below the
530 surface) of the auditory cortex, mice were chronically implanted with a head bar and a circular 4 mm

531 diameter glass window. The implant surgery procedure took place 2-3 weeks following injection of the
532 viral construct. Data acquisition began ~7 days after the implant surgery. Calcium imaging was carried
533 out using a 2-photon laser scanning microscope (B-Scope, Thorlabs, USA). Excitation light of 930 nm
534 (10-50 mW power measured under the objective) was provided by a Mai-Tai eHP (Spectra-Physics,
535 USA) laser fitted with a DeepSee prechirp unit (70 fs pulse width, 80 MHz repetition rate). The laser
536 beam was directed through a Conoptics (CT, USA) modulator and scanned onto the brain with an 8
537 kHz resonant scanner (x-axis) and a galvanometric scan mirror (y-axis), allowing acquisition of 512x512
538 pixel frames at ~30 Hz. Emitted photons were guided through a 525/50 filter onto GaAsP
539 photomultipliers (Hamamatsu, Japan). We used ScanImage[74] to control the microscope during data
540 acquisition and a 16X immersion objective (Nikon, Japan). As with the extracellular recordings under
541 anesthesia, mice were kept anesthetized with a mixture of ketamine and medetomidine throughout
542 the experiment.

543 Viral injections and transgenic expression of proteins for optogenetic control

544 Viral injections were made using the same anesthesia protocol outlined in the previous section. All
545 injections were performed using a custom-made pressure injection system with a calibrated glass
546 pipette positioned in the right hemisphere. The tip of the pipette was carefully and slowly inserted
547 into the area of interest, and ~20 nl boluses were then given every two minutes until the desired
548 volume had been injected. The pipette was then left in position for an additional 5 minutes before
549 being slowly retracted. All optogenetic experiments involving viral injections were carried out >3
550 weeks after the injection to allow for expression of the opsin. All optogenetic stimulation experiments
551 were carried out with a bright white LED shining into the eyes of the mouse throughout the
552 experiment, to saturate photoreceptor responses in the retina and prevent visual activity being
553 induced by the light stimulation[75].

554 *Activating infragranular cells in S1 using ChrimsonR whilst imaging auditory thalamocortical*
555 *axons and boutons*

556 We injected 120 nL of AAV1-CAG-ChrimsonR[76] in S1 (-0.8 and -1.0 mm caudal from bregma, 2.6 mm
557 lateral from midline, and 0.8, 0.65, and 0.5 mm ventral from the cortical surface) to induce expression
558 in the infragranular layers of S1 of C57BL6/J mice. In the same surgery, we also injected AAV1-hSyn-
559 GCaMP6m into auditory thalamus and implanted a glass window over the auditory cortex and a head
560 bar, as explained previously. Finally, in the same surgery, we placed a 400 µm fibre optic cannula on
561 the dura above S1. For optogenetic activation, a 5-7 mW/mm^2, 595 nm LED pulse (Doric Lenses,
562 Canada) was delivered to S1 concurrently with, and for the duration of, broadband noise stimulation
563 (i.e. 50 ms or 200 ms).

564 *Activating RBP4+ cells in layer 5 of S1 using ChR2*

565 We injected 60-80 nl of AAV5-DIO-hChR2-eYFP[77] in S1 (0.8 mm caudal from bregma, 2.6 mm lateral
566 from midline, and 1.0 mm, and 0.95 and 0.9 mm ventral from the cortical surface) of RBP4-cre mice
567 to induce expression of ChR2 in layer 5 neurons. For optogenetic activation, a 5-7 mW/mm^2, 465 nm
568 LED pulse (Doric Lenses) was presented. Light was delivered through a 1 mm fibre acutely positioned
569 on the dura mater above S1 and concurrently with, and for the duration of, sound stimulation (i.e. 50
570 ms).

571 *Suppressing neuronal activity in the auditory sector of thalamic reticular nucleus using Jaws*

572 In order to transfect cells in the auditory sector of TRN (audTRN) with Jaws, we exploited the fact that
573 the MGB in rodents contains very few inhibitory cells[34]. An injection of 140 nL of the cre-dependent
574 retrograde construct pAAV-CAG-FLEX-rc[Jaws-KGC-GFP-ER2][78,79] was placed into the MGB (3.0 mm
575 caudal from bregma, 2.1 mm lateral from midline, 2.8-3.0 mm ventral from the cortical surface) of
576 VGAT-cre mice. The construct did not label cells inside the MGB, but instead induced Jaws expression
577 in cre-expressing TRN cells that project to the injection site in the auditory thalamus. After the
578 injection, we placed a 400 µm fibre optic cannula immediately above audTRN. To maximize the light
579 transmission to the transfected area of audTRN the fibre optic cannula was implanted at a 22.5° angle
580 (relative to the coronal axis). The anatomical position was histologically confirmed after the end of the
581 experiments. For optogenetic suppression, we used a 120 mW/mm^2, 640 nm laser pulse (Toptica
582 Photonics, Germany) of 150 ms length, which started 25 ms before sound onset.

583 *Intersectional targeting and activation of S1-recipient neurons in the shell of the IC*

584 We induced expression of cre in neurons receiving projections from S1, by injecting 200 nL of AA1-
585 hSyn-cre into S1 (-0.8 and -1.0 mm caudal from bregma, 2.6 mm lateral from midline, and 0.9, 0.7, and
586 0.5 mm ventral from the cortical surface). This virus anterogradely and transsynaptically infected
587 neurons receiving projections from S1 and induced expression of cre in those neurons[39]. In order to
588 target expression of ChR2-YFP to IC neurons that receive input from S1, we also injected 200 nL of the
589 cre-dependent construct AAV5-DIO-ChR2-YFP into the lateral part of the IC. For optogenetic
590 activation, a 10 mW/mm^2, 465 nm LED pulse (Doric Lenses) was delivered through a 1 mm optic fiber
591 acutely positioned on the dura mater above the lateral part of the dorsal IC. Stimulation occurred
592 concurrently with, and for the duration of, sound stimulation (i.e. 50 ms).

593 *Suppressing excitatory neurons in S1 using pan-neuronal expression of Jaws*

594 To determine whether S1 is required for whisker-induced suppression of auditory thalamic responses,
595 we injected 380 nL of AAV8-hSyn-Jaws[78] into S1 (-0.8 and -1.0 mm caudal from bregma, 2.6 mm lateral
596 from midline, and 0.9, 0.7, and 0.5 mm ventral from the cortical surface) of mice genetically corrected

597 for age-related hearing loss (C57BL6/NTac.Cdh23[70]). For optogenetic suppression of S1 activity during
598 extracellular recordings in the auditory thalamus, a 5-7 mW/mm^2, 635 nm LED pulse (Doric Lenses)
599 was delivered through an acutely positioned 1 mm optic fibre optic placed on the dura mater above
600 S1. Light stimulation started 10 ms prior to the onset of sound stimulation and lasted 250 ms.

601 *Silencing excitatory cortical activity in VGAT-ChR2-YFP mice*

602 For optogenetic silencing of A1 and S1, we used a blue (465 nm) LED stimulus (duration 150 ms, onset
603 25 ms before auditory and/or somatosensory stimulation) delivered via a 200 µm optic fibre (Doric
604 Lenses) acutely implanted over the dura mater above A1 or the S1 barrel field, respectively. ChR2 was
605 targeted to GABA neurons using VGAT-ChR2-YFP mice. Light power was ~15 mW/mm^2.

606 Histology

607 For post-mortem verification of the electrophysiological recording sites, viral expression pattern, and
608 anatomical tracing, mice were overdosed with pentobarbital (100 mg/Kg body weight, i.p.;
609 pentobarbitone sodium; Merial Animal Health Ltd, Harlow, UK) and perfused transcardially, first with
610 0.1 M phosphate-buffered saline (PBS, pH 7.4) and then with fresh 4% paraformaldehyde (PFA,
611 weight/volume) in PBS. Mice used in anatomical experiments were euthanized and perfused >4 weeks
612 after the virus injections. Mice used for electrophysiology were perfused as soon as the recordings
613 were finished (acute experiments) or when the last recording session was finished (awake recordings),
614 while those used for chronic 2-photon imaging were perfused when all imaging sessions were
615 completed. Following perfusion, the brain was removed from the skull and kept in 4% PFA
616 (weight/volume) in PBS for ~24 hours. The relevant parts of the brains were then sectioned using a
617 vibratome in the coronal plane at a thickness of 50 or 100 µm. Sections were mounted on glass slides
618 and covered in a mounting medium with DAPI (Vectashield, Vector Laboratories). Images were
619 acquired with an Olympus FV1000 confocal laser scanning biological microscope. Confocal images
620 were captured using similar parameters of laser power, gain, pinhole and wavelengths with two
621 channels assigned as the emission color; z-stacks were taken individually for each channel and then
622 collapsed. Images were processed offline using Imaris (Zurich, Switzerland) and ImageJ (NIH, MD,
623 USA).

624

625 Data analysis and statistics

626 We clustered potential neuronal spikes using KiloSort[80] (https://github.com/cortex-lab/KiloSort).
627 Following this automatic clustering step, we manually inspected the clusters in Phy
628 (https://github.com/kwikteam/phy) and removed noise (movement and optogenetic light artefacts).

629 We assessed clusters according to suggested guidelines published by Stephen Lenzi and Nick
630 Steinmetz (https://phy-contrib.readthedocs.io/en/latest/template-gui/#user-guide). Each cluster
631 (following merging and noise removal) was assigned as either noise (clearly not neuronal spike shape),
632 multi-unit (neuronal and mostly consistent spike shape with no absolute refractory period), or single
633 unit (consistent spike shape with absolute refractory period). All analyses performed on the
634 electrophysiological data were run on a combination of small multi-unit clusters and single units (no
635 differences were found between them and therefore we just refer to these as units). Stimulus-evoked
636 responses were measured as the mean firing rate (spikes per second, sp/s) for the duration of the
637 stimulus presentation. Baseline activity was measured from the mean firing rate of the 90 ms
638 preceding stimulus onset.

639 For 2-photon imaging of thalamocortical axons and boutons, we carried out standard
640 preprocessing (e.g. registration of image stacks, region of interest selection, trace extraction) of the
641 calcium data, as described in detail elsewhere[30,81]. Given the slower dynamics of GCaMP6m used to
642 monitor bouton activity from auditory thalamocortical axons, we measured the calcium transient
643 response to a 50 ms stimulus as the mean $\Delta F/F$ over the 16 frames following stimulus onset (i.e. for
644 ~550 ms). Baseline activity was measured as the mean $\Delta F/F$ over the 16 frames preceding stimulus
645 onset.

646 For estimation of somatosensory modulation of noise responses, we only included
647 units/boutons that showed a statistically significant response during sensory stimulation compared to
648 baseline (*t*-test, $P < 0.005$). For estimation of somatosensory modulation of tone responses, we only
649 included units/boutons that showed a statistically significant difference in response among the
650 frequency-level combinations tested (one-way ANOVA, $P < 0.005$).

651 The best frequency (BF) of tone-responsive neurons and boutons was defined as the sound
652 frequency associated with the largest response (i.e. firing rate or $\Delta F/F$, respectively) at the sound level
653 used. For summary statistics and display of summary frequency tuning curves across units/boutons,
654 we normalized the tuning curves of each unit/bouton. To do this, we first estimated the mean
655 frequency tuning curve across conditions (e.g. with and without whisker deflection and/or S1/A1
656 manipulations), and centered the frequency tuning curves for each condition on the BF estimated
657 from the mean frequency tuning curve. We then normalized the response to each tone frequency
658 presented - separately for each condition - by dividing by the response at the BF in the control
659 condition (i.e. tones presented alone). We then produced a summary frequency tuning curve by taking
660 the median of the normalized frequency tuning curves across units/boutons. Error bars for the

661 summary tuning curves were estimated from bootstrapped (10,000 iterations) 95% nonparametric
662 confidence intervals.

663 For group (i.e. across units or boutons) comparisons, we used non-parametric statistical tests
664 (i.e. Wilcoxon signed rank for paired samples and Mann–Whitney *U* test for independent samples).

665 References

666 1. Murray, M. M. & Wallace, M. T. *The neural bases of multisensory processes*. (CRC Press/Taylor
667 & Francis, 2012).

668 2. Diamond, M. E., Von Heimendahl, M., Knutsen, P. M., Kleinfeld, D. & Ahissar, E. 'Where' and
669 'what' in the whisker sensorimotor system. *Nat. Rev. Neurosci.* **9**, 601–612 (2008).

670 3. Wang, X. *et al.* A cross-modality enhancement of defensive flight via parvalbumin neurons in
671 zonal incerta. *Elife* **8**: e42728 (2019).

672 4. Choi, I., Lee, J. Y. & Lee, S. H. Bottom-up and top-down modulation of multisensory integration.
673 *Curr. Opin. Neurobiol.* **52**, 115–122 (2018).

674 5. Bizley, J. K., Nodal, F. R., Bajo, V. M., Nelken, I. & King, A. J. Physiological and anatomical
675 evidence for multisensory interactions in auditory cortex. *Cereb. Cortex* **17**, 2172–2189 (2007).

676 6. Rao, R. P., Mielke, F., Bobrov, E. & Brecht, M. Vocalization-whisking coordination and
677 multisensory integration of social signals in rat auditory cortex. *Elife* **3**, e03185 (2014).

678 7. Meredith, M. A. & Allman, B. L. Single-unit analysis of somatosensory processing in the core
679 auditory cortex of hearing ferrets. *Eur. J. Neurosci.* **41**, 686–698 (2015).

680 8. Kayser, C., Petkov, C. I. & Logothetis, N. K. Visual modulation of neurons in auditory cortex.
681 *Cereb. Cortex* **18**, 1560–1574 (2008).

682 9. Rockland, K. S. & Ojima, H. Multisensory convergence in calcarine visual areas in macaque
683 monkey. *Int. J. Psychophysiol.* **50**, 19–26 (2003).

684 10. Cappe, C. & Barone, P. Heteromodal connections supporting multisensory integration at low
685 levels of cortical processing in the monkey. *Eur. J. Neurosci.* **22**, 2886–2902 (2005).

686 11. Budinger, E., Heil, P., Hess, A. & Scheich, H. Multisensory processing via early cortical stages:
687 Connections of the primary auditory cortical field with other sensory systems. *Neuroscience*

688 **143**, 1065–1083 (2006).

689 12. Banks, M. I., Uhlrich, D. J., Smith, P. H., Krause, B. M. & Manning, K. A. Descending projections
690 from extrastriate visual cortex modulate responses of cells in primary auditory cortex. *Cereb.*
691 *Cortex* **21**, 2620–2638 (2011).

692 13. Stehberg, J., Stehberg, J., Dang, P. T. & Frostig, R. D. Unimodal primary sensory cortices are
693 directly connected by long-range horizontal projections in the rat sensory cortex. *Front.*
694 *Neuroanat.* **8**, 1–19 (2014).

695 14. Zingg, B. *et al.* Neural networks of the mouse neocortex. *Cell* **156**, 1096–1111 (2014).

696 15. Iurilli, G. *et al.* Sound-driven synaptic inhibition in primary visual cortex. *Neuron* **73**, 814–828
697 (2012).

698 16. Ibrahim, L. A. *et al.* Cross-modality sharpening of visual cortical processing through layer-1-
699 mediated inhibition and disinhibition. *Neuron* **89**, 1031–1045 (2016).

700 17. Song, Y.-H. *et al.* A neural circuit for auditory dominance over visual perception. *Neuron* **93**,
701 940–954 (2017).

702 18. Atilgan, H. *et al.* Integration of visual information in auditory cortex promotes auditory scene
703 analysis through multisensory binding. *Neuron* **97**, 640–655 (2018).

704 19. Kimura, A. & Imbe, H. Robust subthreshold cross-modal modulation of auditory response by
705 cutaneous electrical stimulation in first- and higher-order auditory thalamic nuclei.
706 *Neuroscience* **372**, 161–180 (2018).

707 20. Wu, C., Stefanescu, R. A., Martel, D. T. & Shore, S. E. Listening to another sense: somatosensory
708 integration in the auditory system. *Cell Tissue Res.* **361**, 233–250 (2015).

709 21. Chou, X. L. *et al.* Contextual and cross-modality modulation of auditory cortical processing
710 through pulvinar mediated suppression. *Elife* **9**, e54157 (2020).

711 22. Khorevin, V. I. Effect of electrodermal stimulation on single unit responses to acoustic
712 stimulation in the parvocellular part of the medial geniculate body. *Neurophysiology* **12**, 129–
713 134 (1980).

714 23. Sherman, S. M. & Guillery, R. W. Distinct functions for direct and transthalamic corticocortical
715 connections. *J. Neurophysiol.* **106**, 1068–1077 (2011).

716 24. Lohse, M., Bajo, V. M. & King, A. J. Development, organization and plasticity of auditory circuits:
717 Lessons from a cherished colleague. *Eur. J. Neurosci.* **49**, 990–1004 (2019).

718 25. Fu, K. G. *et al.* Auditory cortical neurons respond to somatosensory stimulation. *J. Neurosci.* **23**,
719 7510–7515 (2003).

720 26. Kayser, C., Petkov, C. I., Augath, M. & Logothetis, N. K. Integration of touch and sound in
721 auditory cortex. *Neuron* **48**, 373–384 (2005).

722 27. Zhang, M., Kwon, S. E., Ben-Johny, M., O'Connor, D. H. & Issa, J. B. Spectral hallmark of
723 auditory-tactile interactions in the mouse somatosensory cortex. *Commun. Biol.* **3**, 1–17
724 (2020).

725 28. Lu, E., Llano, D. A. & Sherman, S. M. Different distributions of calbindin and calretinin
726 immunostaining across the medial and dorsal divisions of the mouse medial geniculate body.
727 *Hear. Res.* **257**, 16–23 (2009).

728 29. Anderson, L. A. & Linden, J. F. Physiological differences between histologically defined
729 subdivisions in the mouse auditory thalamus. *Hear. Res.* **274**, 48–60 (2011).

730 30. Vasquez-Lopez, S. A. *et al.* Thalamic input to auditory cortex is locally heterogeneous but
731 globally tonotopic. *Elife* **6**, e25141 (2017).

732 31. Takesian, A. E., Bogart, L. J., Lichtman, J. W. & Hensch, T. K. Inhibitory circuit gating of auditory
733 critical-period plasticity. *Nat. Neurosci.* **21**, 218–227 (2018).

734 32. Allen, A. E., Procyk, C. A., Brown, T. M. & Lucas, R. J. Convergence of visual and whisker
735 responses in the primary somatosensory thalamus (ventral posterior medial region) of the
736 mouse. *J. Physiol.* **595**, 865–881 (2017).

737 33. Mo, C. & Sherman, S. M. A sensorimotor pathway via higher-order thalamus. *J. Neurosci.*
738 (2018).

739 34. Winer, J. A. & Larue, D. T. Evolution of GABAergic circuitry in the mammalian medial geniculate
740 body. *Proc Natl Acad Sci U S A* **93**, 3083–3087 (1996).

741 35. Kimura, A., Yokoi, I., Imbe, H., Donishi, T. & Kaneoke, Y. Auditory thalamic reticular nucleus of
742 the rat: Anatomical nodes for modulation of auditory and cross-modal sensory processing in
743 the loop connectivity between the cortex and thalamus. *J. Comp. Neurol.* **520**, 1457–1480
744 (2012).

745 36. Lesicko, A. M. H., Hristova, T. S., Maigler, K. C. & Llano, D. A. Connectional modularity of top-
746 down and bottom-up multimodal inputs to the lateral cortex of the mouse inferior colliculus.
747 *J. Neurosci.* **36**, 11037–11050 (2016).

748 37. Clarke, B. A. & Lee, C. C. Inhibitory projections in the mouse auditory tectothalamic system.
749 *Brain Sci.* **8**, (2018).

750 38. Beebe, N. L., Mellott, J. G. & Schofield, B. R. Inhibitory projections from the inferior colliculus
751 to the medial geniculate body originate from four subtypes of GABAergic Cells. *eNeuro* **5**, 1–13
752 (2018).

753 39. Zingg, B. *et al.* AAV-mediated anterograde transsynaptic tagging: Mapping corticocollicular
754 input-defined neural pathways for defense behaviors. *Neuron* **93**, 33–47 (2017).

755 40. Ghazanfar, A. A., Maier, J. X., Hoffman, K. L. & Logothetis, N. K. Multisensory integration of
756 dynamic faces and voices in rhesus monkey auditory cortex. *J. Neurosci.* **25**, 5004–5012 (2005).

757 41. Lakatos, P., Chen, C., Connell, M. N. O., Mills, A. & Schroeder, C. E. Neuronal oscillations and
758 multisensory interaction in primary auditory cortex. *Neuron* **53**, 279–292 (2007).

759 42. Perrodin, C., Kayser, C., Logothetis, N. K. & Petkov, C. I. Natural asynchronies in audiovisual
760 communication signals regulate neuronal multisensory interactions in voice-sensitive cortex.
761 *Proc. Natl. Acad. Sci. U. S. A.* **112**, 273–278 (2015).

762 43. De La Mothe, L. A., Blumell, S., Kajikawa, Y. & Hackett, T. A. Thalamic connections of the
763 auditory cortex in marmoset monkeys: Core and medial belt regions. *J. Comp. Neurol.* **496**, 72–
764 96 (2006).

765 44. Smiley, J. F. & Falchier, A. Multisensory connections of monkey auditory cerebral cortex. *Hear.*
766 *Res.* **258**, 37–46 (2009).

767 45. Avillac, M., Ben Hamed, S. & Duhamel, J.-R. Multisensory integration in the ventral intraparietal
768 area of the macaque monkey. *J. Neurosci.* **27**, 1922–1932 (2007).

769 46. Ohshiro, T., Angelaki, D. E. & Deangelis, G. C. A normalization model of multisensory
770 integration. *Nat. Neurosci.* **14**, 775–782 (2011).

771 47. Ohshiro, T., Angelaki, D. E. & DeAngelis, G. C. A neural signature of divisive normalization at the
772 Level of multisensory integration in primate cortex. *Neuron* **95**, 399–411 (2017).

773 48. Bartlett, E. L. & Smith, P. H. Anatomic, intrinsic, and synaptic properties of dorsal and ventral

774 division neurons in rat medial geniculate body. *J. Neurophysiol.* **81**, 1999–2016 (1999).

775 49. Wepsic, J. G. Multimodal sensory activation of cells in the magnocellular medial geniculate
776 nucleus. *Exp. Neurol.* **15**, 299–318 (1966).

777 50. Bordi, F. & LeDoux, J. E. Response properties of single units in areas of rat auditory thalamus
778 that project to the amygdala - I. Acoustic discharge patterns and frequency receptive fields.
779 *Exp. Brain Res.* **98**, 261–274 (1994).

780 51. Jones, E. G. & Burton, H. Cytoarchitecture and somatic sensory connectivity of thalamic nuclei
781 other than the ventrobasal complex in the cat. *J. Comp. Neurol.* **154**, 395–432 (1974).

782 52. Lund, R. D. & Webster, K. E. Thalamic afferents from the spinal cord and the trigeminal nucleus.
783 An experiment anatomic study in the rat. *J. Comp. Neurol.* **130**, 313–328 (1967).

784 53. Lund, R. D. & Webster, K. E. Thalamic afferents from the dorsal column nuclei. An experimental
785 anatomical study in the rat. *J. Comp. Neurol.* **130**, 301–311 (1967).

786 54. Doron, N. N. & Ledoux, J. E. Cells in the posterior thalamus project to both amygdala and
787 temporal cortex: A quantitative retrograde double-labeling study in the rat. *J. Comp. Neurol.*
788 **425**, 257–274 (2000).

789 55. Huang, C. L. & Winer, J. A. Auditory thalamocortical projections in the cat: Laminar and areal
790 patterns of input. *J. Comp. Neurol.* **427**, 302–331 (2000).

791 56. Moriizumi, T. & Hattori, T. Ultrastructural morphology of projections from the medial
792 geniculate nucleus and its adjacent region to the basal ganglia. *Brain Res. Bull.* **29**, 193–198
793 (1992).

794 57. Barsy, B. *et al.* Associative and plastic thalamic signaling to the lateral amygdala controls fear
795 behavior. *Nat. Neurosci.* 1–13 (2020). doi:10.1038/s41593-020-0620-z

796 58. Cruikshank, S. J., Edeline, J. M. & Weinberger, N. M. Stimulation at a site of auditory-
797 somatosensory convergence in the medial geniculate nucleus is an effective unconditioned
798 stimulus for fear conditioning. *Behav Neurosci* **106**, 471–483 (1992).

799 59. Weinberger, N. M. The medial geniculate, not the amygdala, as the root of auditory fear
800 conditioning. *Hear. Res.* **274**, 61–74 (2011).

801 60. Smith, P. H., Bartlett, E. L. & Kowalkowski, A. Unique combination of anatomy and physiology
802 in cells of the rat paralaminar thalamic nuclei adjacent to the medial geniculate body. *J. Comp.*

803 *Neurol.* **496**, 314–334 (2006).

804 61. Bajo, V. M. & King, A. J. Cortical modulation of auditory processing in the midbrain. *Front.*
805 *Neural Circuits* **6**, 1–12 (2013).

806 62. Guo, W., Clause, A. R., Barth-Maron, A. & Polley, D. B. A corticothalamic circuit for dynamic
807 switching between feature detection and discrimination. *Neuron* **95**, 180–194 (2017).

808 63. Zhang, Z. *et al.* Corticofugal projection inhibits the auditory thalamus through the thalamic
809 reticular nucleus. *J. Neurophysiol.* **99**, 2938–2945 (2008).

810 64. Shore, S. E. & Zhou, J. Somatosensory influence on the cochlear nucleus and beyond. *Hear. Res.*
811 **216**–**217**, 90–99 (2006).

812 65. Aitkin, L. M., Kenyon, C. E. & Philpott, P. The representation of the auditory and somatosensory
813 systems in the external nucleus of the cat inferior colliculus. *J. Comp. Neurol.* **196**, 25–40
814 (1981).

815 66. Peruzzi, D., Bartlett, E., Smith, P. H. & Oliver, D. L. A monosynaptic GABAergic input from the
816 inferior colliculus to the medial geniculate body in rat. *J. Neurosci.* **17**, 3766–77 (1997).

817 67. Winer, J. A., Mariet, R. L. Saint, Larue, D. T. & Oliver, D. L. GABAergic feedforward projections
818 from the inferior colliculus to the medial geniculate body. **93**, 8005–8010 (1996).

819 68. Kayser, C., Logothetis, N. K. & Panzeri, S. Visual enhancement of the information
820 representation in auditory cortex. *Curr. Biol.* **20**, 19–24 (2010).

821 69. Otazu, G. H., Tai, L. H., Yang, Y. & Zador, A. M. Engaging in an auditory task suppresses
822 responses in auditory cortex. *Nat. Neurosci.* **12**, 646–654 (2009).

823 70. Mianné, J. *et al.* Correction of the auditory phenotype in C57BL/6N mice via CRISPR/Cas9-
824 mediated homology directed repair. *Genome Med.* **8**, 1–12 (2016).

825 71. Stiebler, I. & Ehret, G. Inferior colliculus of the house mouse. I. A quantitative study of tonotopic
826 organization, frequency representation, and tone-threshold distribution. *J. Comp. Neurol.* **238**,
827 65–76 (1985).

828 72. Portfors, C. V., Mayko, Z. M., Jonson, K., Cha, G. F. & Roberts, P. D. Spatial organization of
829 receptive fields in the auditory midbrain of awake mouse. *Neuroscience* **193**, 429–439 (2011).

830 73. Guo, W. *et al.* Robustness of cortical topography across fields, laminae, anesthetic states, and

831 neurophysiological signal types. *J. Neurosci.* **32**, 9159–9172 (2012).

832 74. Pologruto, T. A., Sabatini, B. L. & Svoboda, K. ScanImage: Flexible software for operating laser
833 scanning microscopes. *Biomed. Eng. Online* **2**, 1–9 (2003).

834 75. Danskin, B. *et al.* Optogenetics in mice performing a visual discrimination task: Measurement
835 and suppression of retinal activation and the resulting behavioral artifact. *PLoS One* **10**, 1–13
836 (2015).

837 76. Klapoetke, N. C. *et al.* Independent optical excitation of distinct neural populations. *Nat.*
838 *Methods* **11**, 338–346 (2014).

839 77. Nagel, G. *et al.* Channelrhodopsin-2, a directly light-gated cation-selective membrane channel.
840 *Proc. Natl. Acad. Sci.* **100**, 13940–13945 (2003).

841 78. Chuong, A. S. *et al.* Noninvasive optical inhibition with a red-shifted microbial rhodopsin. *Nat.*
842 *Neurosci.* **17**, 1123–1129 (2014).

843 79. Tervo, D. G. R. *et al.* A designer AAV variant permits efficient retrograde access to projection
844 neurons. *Neuron* **92**, 372–382 (2016).

845 80. Pachitariu, M., Steinmetz, N. A., Kadir, S., Carandini, M. & Harris, K. D. Kilosort: realtime spike-
846 sorting for extracellular electrophysiology with hundreds of channels.
847 http://www.biorxiv.org/content/10.1101/061481v1 (2016). doi:10.1101/061481

848 81. Barnstedt, O., Keating, P., Weissenberger, Y., King, A. J. & Dahmen, J. C. Functional
849 microarchitecture of the mouse dorsal inferior colliculus revealed through in vivo two-photon
850 calcium imaging. *J. Neurosci.* **35**, 10927–10939 (2015).

851